

Transfer printing of graphene strip from the graphene grown on copper wires

This article has been downloaded from IOPscience. Please scroll down to see the full text article.

2011 Nanotechnology 22 185309

(<http://iopscience.iop.org/0957-4484/22/18/185309>)

View [the table of contents for this issue](#), or go to the [journal homepage](#) for more

Download details:

IP Address: 140.113.77.61

The article was downloaded on 23/03/2011 at 03:46

Please note that [terms and conditions apply](#).

Transfer printing of graphene strip from the graphene grown on copper wires

Ching-Yuan Su¹, Dongliang Fu, Ang-Yu Lu, Keng-Ku Liu, Yanping Xu, Zhen-Yu Juang and Lain-Jong Li

Research Center for Applied Sciences, Academia Sinica, Taipei 11529, Taiwan

E-mail: cysu@gate.sinica.edu.tw

Received 13 December 2010, in final form 18 February 2011

Published 22 March 2011

Online at stacks.iop.org/Nano/22/185309

Abstract

A simple, cost-effective and lithography-free fabrication of graphene strips for device applications is demonstrated. The graphene thin layers were directly grown on Cu wires, followed by Cu etching and transfer printing to arbitrary substrates by a PDMS stamp. The Cu wires can be arranged on the PDMS stamp in a desired pattern; hence, the substrates can receive graphene strips with the same pattern. Moreover, the preparation of graphene strips does not involve conventional lithography; therefore, the surface of the graphene strip is free of residual photoresists, which may be useful for studies requiring clean graphene surfaces.

 Online supplementary data available from stacks.iop.org/Nano/22/185309/mmedia

(Some figures in this article are in colour only in the electronic version)

1. Introduction

Graphene has attracted much attention not only because of its perfect two-dimensional carbon crystalline structure, which enables the explorations of fundamental physics, but also due to its exciting potential in post-silicon electronics [1–6]. Its unique physical properties, such as high intrinsic carrier mobility ($\sim 200\,000\text{ cm}^2\text{ V}^{-1}\text{ s}^{-1}$) [7], quantum electronic transport [2, 3], tunable band gap [4, 8], high mechanical strength and elasticity [9], and superior thermal conductivity [10], make graphene promising for many applications, including high speed transistors [11–15], transparent conductive thin films [15–20], energy/thermal management [21, 10], and chemical/biological sensors [22–27]. The device application of graphene requires versatile patterns such as strips, ribbons or other defined shapes for electrical transport. Nevertheless, conventional lithographic patterning is expensive and time consuming. Also, the standard lithographic processes typically involve the use of polymethylmethacrylate (PMMA) photoresists on graphene surface, which introduces considerable n-type doping [28] and contamination causing carrier scattering [26, 29]. Moreover, PMMA is typically used as the supporting layer for the transfer of chemical vapor deposition (CVD) produced graphene onto the desired substrates. Although a recent work [29] has demonstrated

that using a high temperature ($\sim 400^\circ\text{C}$) cleaning process in a H_2/Ar atmosphere can remove most of the photoresists, the possible remaining residues may still hinder applications, such as sensors, that require clean surfaces. Therefore, researchers have started to investigate lithography-free approaches for graphene patterning, for example, by using quartz filament as a shadow mask to define the graphene [30]. Here we present a simple, cost-effective, lithography-free fabrication of graphene strips for device applications. The graphene thin layers were directly grown on Cu wires, followed by Cu etching and transfer printing to arbitrary substrates by a poly(dimethylsiloxane) (PDMS) stamp. The obtained strips can be used as a transistor for macroelectronics or a sensor, as demonstrated in the text.

2. Experimental details

2.1. CVD growth of graphene on Cu wire

For the CVD growth of graphene on Cu wires, high purity copper micro-wire (99.9% deom Nilaco Co.; $50\ \mu\text{m}$ in diameter) was put on a quartz plate and then loaded into the center of a tubular furnace (TF55030, Lindberg/Blue/M). The chamber was evacuated to $\sim 5\text{ mTorr}$ and the temperature was increased from room temperature to 1000°C . Prior to growth, a pretreatment step was performed by flowing a diluted

¹ Author to whom any correspondence should be addressed.

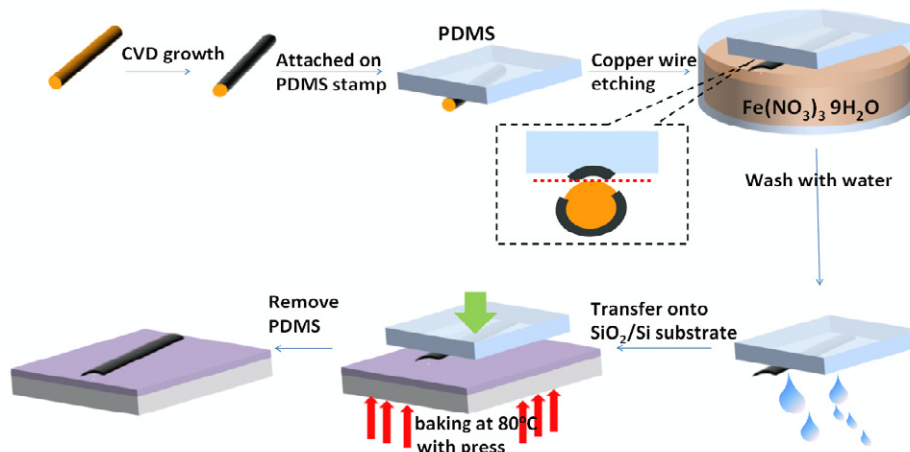


Figure 1. Schematic illustration for the preparation of CVD graphene strips, where the Cu wire with CVD-grown graphene on surfaces was directly put on a PDMS stamp. The subsequent Cu etching removes the Cu wire and leaves long and narrow graphene strips on the PDMS that can be used for device applications.

hydrogen gas (H_2/Ar : 5 sccm/400 sccm at 500 Torr) through the chamber for 30 min. During the growth step, a gas mixture of methane and hydrogen ($\text{CH}_4/\text{H}_2 = 5 \text{ sccm}/30 \text{ sccm}$) was introduced and the pressure was controlled at 450 mTorr for 20 min. The system was then cooled down (cooling rate $\sim 5^\circ\text{C s}^{-1}$) to room temperature to complete the growth.

2.2. Transfer printing of graphene strips

To transfer print the as-grown graphene layers onto the substrate, the Cu wire after CVD growth was put on a cleaned PDMS elastomer and flattened with a glass plate. The Cu wires were then securely attached on the surface of the PDMS. After that, the Cu wire attached PDMS was then flipped over and immersed in $\text{Fe}(\text{NO}_3)_3 \cdot 9\text{H}_2\text{O}$ (4.76 wt%) overnight. The PDMS was then immersed in deionized (DI) water to dilute and remove the etchant and residues. The graphene strips were then transferred onto the desired substrate by pressing the PDMS onto the substrates at 80°C for 30 min. The graphene strips were then obtained after the PDMS was delaminated from the substrate.

2.3. Device fabrication

The field effect transistor was fabricated by evaporating a Au electrode (30 nm thick) directly on top of the as-printed graphene strips using a copper grid (200 mesh, $20 \mu\text{m}$ spacing) as a hard mask. To make the pH sensor device, silver paint was deposited on the two terminals of the printed graphene strip. To ensure the sensing property is directly from the reaction between the probe solution and graphene, the graphene-electrode junctions were blocked by PDMS. When carrying out the sensing study, the Ag electrode was used as a gate electrode and was immersed in solutions with various pH values, prepared by mixing the required ratio of $\text{KOH}_{(\text{aq})}$ and $\text{H}_2\text{SO}_{4(\text{aq})}$. A commercially available pH meter (HCT-201U) was used to measure the pH value of solutions.

2.4. Characterizations and electrical measurements

The atomic force microscopy (AFM) images were performed in a Veeco Dimension-Icon system. Raman spectra were collected in a NT-MDT confocal Raman microscopic system (laser wavelength 473 nm and laser spot size is $\sim 0.4 \mu\text{m}$). The Si peak at 520 cm^{-1} was used as reference for wavenumber calibration. All electrical measurement were performed in ambient conditions using a Keithley semiconductor parameter analyzer (model: 4200-SCS).

3. Results and discussion

Large-area and thin-layer graphene films have been successfully synthesized on Cu or Ni substrates using CVD methods [31–36]. In this communication, we used Cu wire with a diameter $\sim 50 \mu\text{m}$ as a template for growing CVD graphene layers. After thin graphene layers were grown on long Cu wires, these Cu wires were put on a PDMS stamp followed by pressing to securely fix them on PDMS. The Cu wires were then subjected to an etching solution $\text{Fe}(\text{NO}_3)_3 \cdot 9\text{H}_2\text{O}$ that efficiently dissolved Cu wires and simultaneously removed the graphene films which were either loosely or not contacted with the PDMS stamp. It is notable that although the CVD-grown graphene film cover the whole surface of Cu wire, it is inevitable that the major part of the graphene will be removed in the etching step. As shown in figure 1, the etching process leaves only the graphene strips which closely adhere to the PDMS surface, and the typical width of the obtained strips is around $10\text{--}30 \mu\text{m}$, smaller than the initial diameter of the Cu wires ($\sim 50 \mu\text{m}$). The graphene strips obtained can be subsequently transferred onto arbitrary substrates with the PDMS stamp at 80°C . The substrate 300 nm SiO_2 on Si was used to receive the graphene strips in our study. Note that due to the PDMS being fully cured before contacting graphene for transfer, less residues are anticipated, compared with the commonly used PMMA-assisted transfer processes. These processes allow us to obtain graphene strips with lengths up to 0.5 mm while the width can be varied from

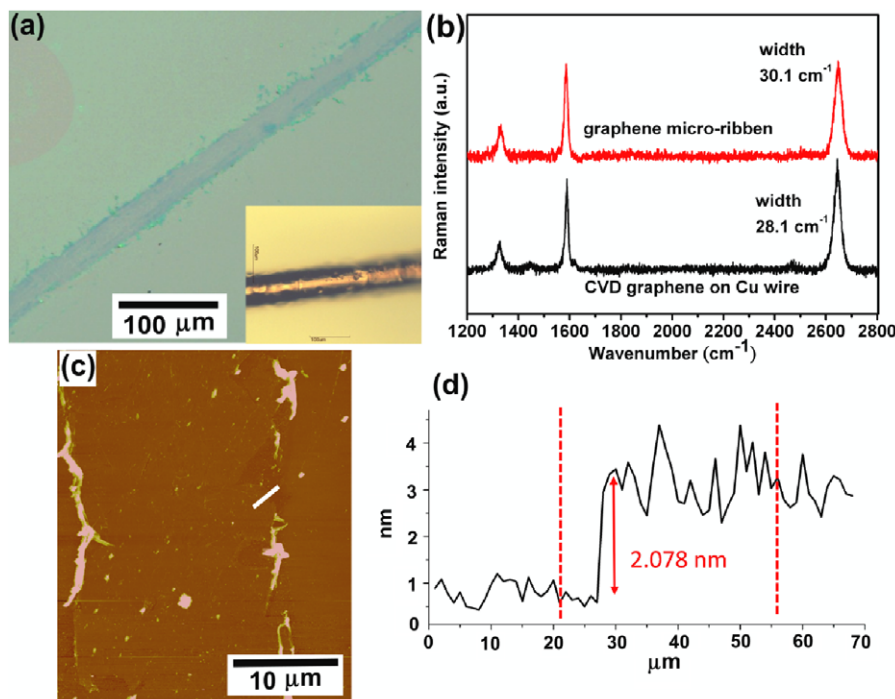


Figure 2. (a) Optical image for a graphene strip transferred onto 300 nm of SiO₂/Si substrate from a copper wire (inset) deposited with CVD graphene. (b) Raman spectra for the graphene ribbon before and after transferring onto the SiO₂/Si substrate. (c) The AFM image of the transferred graphene strip. (d) The height profile of the corresponding AFM image, where the height measurement along the indicated solid line (from right to left) in (c) shows that the graphene thickness is ~ 2 nm.

10 to 45 μm , depending on the diameter of the Cu wires (see figure S1 in supporting materials available at stacks.iop.org/Nano/22/185309/mmedia).

Figure 2(a) shows the optical image of the transferred graphene strips on 300 nm SiO₂/Si and the inset demonstrates the optical image taken for the Cu wire before Cu etching. Figure 2(b) shows the typical Raman spectrum for the CVD graphene grown on Cu wires and that for the transferred graphene strip. The well-known G peak (at $\sim 1585\text{ cm}^{-1}$) and 2D peak (at $\sim 2700\text{ cm}^{-1}$) are characteristic peaks of graphene [37]. The sharp line width ($\sim 30\text{ cm}^{-1}$) of the 2D peak indicate that the as-grown and transferred graphene is within few layers. It is noted that the correlation between 2D width (or 2D line shape) and number of graphene layers is only valid in A–B stacked graphene [38] and therefore this does not allow one to identify the number of layers for CVD graphene. Nevertheless, it has been reported that the peak intensity ratio between 2D and G, $I(2D)/I(G)$, provides a good estimation for the number of layers in CVD graphene [35, 36]. The Raman $I(2D)/I(G)$ ratio in figure 2(b) implies that bilayered graphene was initially grown on this copper wire and the transferred graphene strip also had the same number of layers. In addition, the ratio of the integrated peak area between D and G bands, $A(D)/A(G)$, has been used to indicate the defect level in graphene [35]. The increase of the $A(D)/A(G)$ after etching and transfer (Raman spectra in figure 2(b)) suggests that the etching and transfer processes introduce some defects to graphene. Figures 2(c) and (d) show the AFM image and the height profile respectively for the obtained graphene strip. The measured thickness for the ribbon

was ~ 2.08 nm, corroborating the conclusion from Raman measurements that the graphene is few layers. The AFM image also reveals that the transferred strip is a continuous film. From the AFM images it can be seen that some graphene wrinkles and residues were unavoidably obtained at the surface and edge of the strip (see the high resolution AFM image shown in figure S2 available at stacks.iop.org/Nano/22/185309/mmedia). Meanwhile, the number of graphene layers in the strip is dominated by the as-grown graphene on copper wire. Thus, the number of graphene layers of the strip can be adjusted by controlling the growth of CVD graphene on copper wires. Strips with single-layer graphene are also frequently obtained in our study. However, the transferred single-layered strip exhibits poorer continuity compared to bilayered or few-layered graphene.

Figure 3(a) demonstrates the typical output characteristics (drain current I_d versus drain voltage V_d) for the graphene strip device. The inset shows the photographic top view of the device, where the graphene edge is indicated by dotted lines. Figure 3(b) shows the transfer curves (I_d versus gate voltage V_g) for the corresponding device. The field effect mobility of holes was extracted based on the slope $\Delta I_d/\Delta V_g$ fitted to the linear regime of the transfer curves using the equation $\mu = (L/WC_{\text{ox}}V_d)(\Delta I_d/\Delta V_g)$, where L and W are the channel length and width, and C_{ox} the gate capacitance. The field effect mobility of this particular transfer-printed graphene strip goes up to $\sim 873\text{ cm}^2\text{ V}^{-1}\text{ s}^{-1}$ in ambient measurement conditions. Note that the heavy p-doping of graphene is mainly due to the metal ion residue (i.e., Fe ion contained due to the Cu etching step), which can be

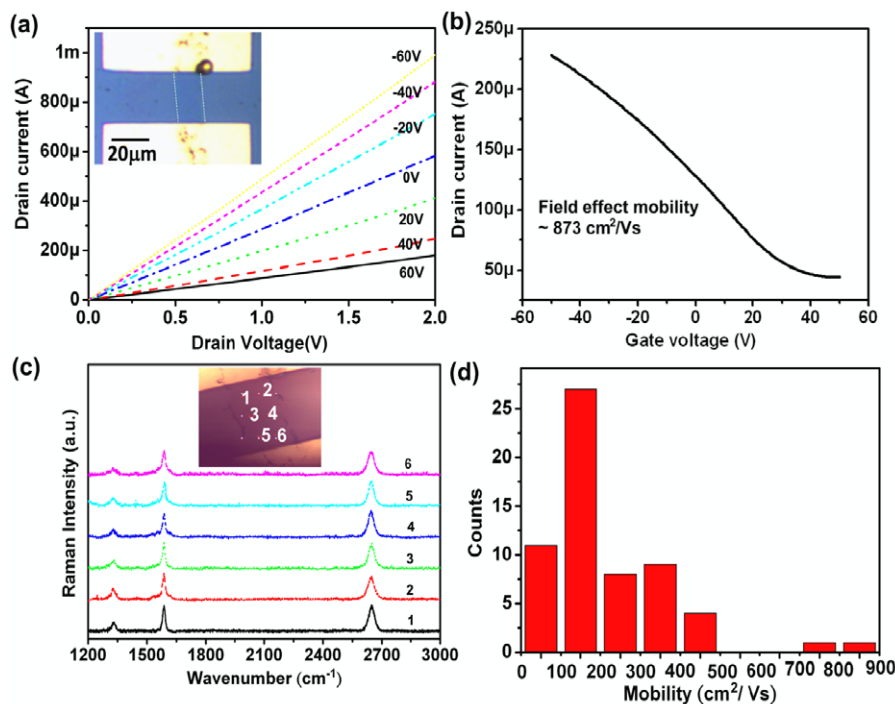


Figure 3. (a) Typical output characteristics (drain current I_d versus drain voltage V_d) for a transistor device based on a bilayered graphene strip. (b) Transfer characteristics for a transistor device based on a bilayered graphene strip. (c) Raman spectra on corresponding device. (d) The statistical mobility data for the devices made from 61 graphene strips.

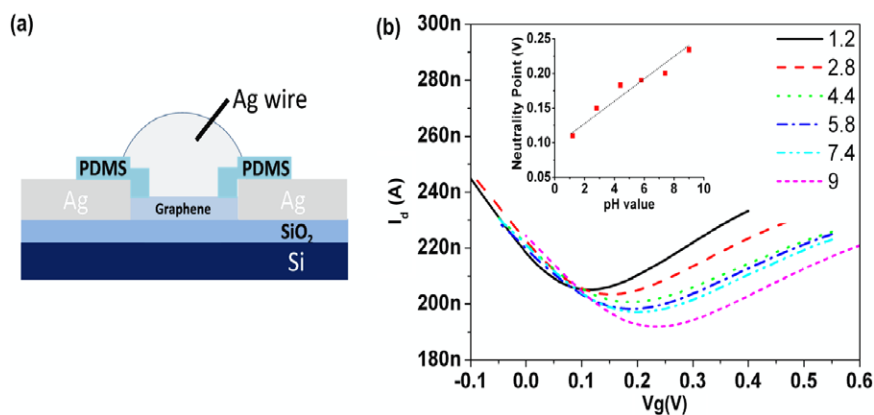


Figure 4. (a) Schematic illustration of a graphene-based pH sensor made by transferred graphene strip. (b) The transfer curves of the graphene strip operated by liquid gating, showing that the device is sensitive to the pH values of the solution.

improved by repeated washing with diluted acid and DI water (see supporting material figure S3 available at stacks.iop.org/Nano/22/185309/mmedia for detail). The Raman spectra in figure 3(c) on this graphene suggest that the graphene strip has good uniformity. In addition, figure 3(d) summarizes the statistical mobility data for the 61 devices measured (all graphene strips on these devices have thicknesses from 1.6 to 2.0 nm measured by AFM). The statistical result clearly demonstrates that a fairly high percentage ($\sim 81\%$) of devices exhibit mobilities higher than $100 \text{ cm}^2 \text{ V}^{-1} \text{ s}^{-1}$, suggesting that they could be used for electronic device applications, especially for flexible electronics due to the advantage of the higher bending limit in graphene.

To demonstrate the feasibility of using these devices for wider applications, such as sensing in solutions, we operate the devices with liquid gating. Silver paint was used as source and drain electrodes and PDMS was applied to block the graphene–electrode junctions, thus avoiding electrical shorts between gate and source/drain electrodes [22, 39, 40]. The device is gated through a Ag/AgCl reference electrode inserted in the electrolyte, as shown in figure 4(a). The transfer curves displayed in figure 4(b) are sensitive to the pH values of the solutions. The inset shows the gate voltage corresponding to the neutrality point of each curve plotted as a function of the pH. The trend (positive shift of neutrality point with increasing pH) is consistent with the reports by other groups,

where the sensors were made from mechanical exfoliation [41] and epitaxial graphene [42]. Moreover, the sensitivity of the pH sensor made by our CVD-grown graphene ($\Delta V/\Delta \text{pH} \sim 0.022$) is comparable to these made from mechanical exfoliated graphene (~ 0.025) [41]. This suggests that the developed lithography-free approach allow us to obtain a high-sensitivity sensor due to the good quality of the graphene, which could pave the way toward low-cost and flexible devices in many applications.

4. Conclusions

In this work, we have demonstrated that graphene layers can be grown on the surface of thin Cu wires. Long graphene strips can be transferred to arbitrary substrates by the proposed transfer printing method. It is noted that the Cu wires can be arranged on the PDMS stamp in a desired pattern; hence, the substrates can receive graphene strips with the same pattern. Moreover, the preparation of graphene strips does not involve conventional lithography; therefore, the surface of the graphene strip is free of residual photoresists, which may be useful for studies requiring clean graphene surfaces. Moreover, the obtained strips can be used in transistors for microelectronics or as sensor components.

Acknowledgments

This research was supported by Academia Sinica and National Science Council Taiwan (NSC-99-2112-M-001-021-MY3 and 99-2738-M-001-001).

References

- [1] Novoselov K S, Geim A K, Morozov S V, Zhang Y, Dubonos S V, Grigorieva I V and Firsov A A 2004 Electric field effect in atomically thin carbon films *Science* **306** 666
- [2] Novoselov K S, Geim A K, Morozov S V, Jiang D, Katsnelson M I, Grigorieva I V, Dubonos S V and Firsov A A 2005 Two-dimensional gas of massless Dirac fermions in graphene *Nature* **438** 197
- [3] Zhang Y, Tan Y W, Stormer H L and Kim P 2005 Experimental observation of the quantum Hall effect and Berry's phase in graphene *Nature* **438** 201
- [4] Han M Y, Ozyilmaz B, Zhang Y and Kim P 2007 Energy band-gap engineering of graphene nanoribbons *Phys. Rev. Lett.* **98** 206805
- [5] Oostinga J B, Heersche H B, Liu X L, Morpurgo A F and Vandersypen L M K 2008 Gate-induced insulating state in bilayer graphene devices *Nat. Mater.* **7** 7151
- [6] Schedin F, Geim A K, Morozov S V, Hill E W, Blake P, Katsnelson M I and Novoselov K S 2007 Detection of individual gas molecules adsorbed on graphene *Nat. Mater.* **6** 652
- [7] Bolotin K I, Sikes K J, Jiang Z, Klima M, Fudenberg G, Hone J, Kim P and Stormer H L 2008 Ultrahigh electron mobility in suspended graphene *Solid State Commun.* **146** 351
- [8] Zhang Y B, Tang T T, Girit C, Hao Z, Martin M C, Zettl A, Crommie M F, Shen Y R and Wang F 2009 Direct observation of a widely tunable bandgap in bilayer graphene *Nature* **459** 820
- [9] Lee C, Wei X D, Kysar J W and Hone J 2008 Measurement of the elastic properties and intrinsic strength of monolayer graphene *Science* **321** 385
- [10] Balandin A A, Ghosh S, Bao W Z, Calizo I, Teweldebrhan D, Miao F and Lau C N 2008 Superior thermal conductivity of single-layer graphene *Nano Lett.* **8** 902
- [11] Chen Z H, Lin Y M, Rooks M J and Avouris P 2007 Graphene nano-ribbon electronics *2nd Int. Symp. on Nanometer-scale Quantum Physics (Tokyo)*
- [12] Lemme M C, Echtermeyer T J, Baus M and Kurz H 2007 A graphene field-effect device *IEEE Electron Device Lett.* **28** 282
- [13] Martin J, Akerman N, Ulbricht G, Lohmann T, Smet J H, Von Klitzing K and Yacoby A 2008 Observation of electron-hole puddles in graphene using a scanning single-electron transistor *Nat. Phys.* **4** 144
- [14] Das A *et al* 2008 Monitoring dopants by Raman scattering in an electrochemically top-gated graphene transistor *Nat. Nanotechnol.* **3** 210
- [15] Eda G, Fanchini G and Chhowalla M 2008 Large-area ultrathin films of reduced graphene oxide as a transparent and flexible electronic material *Nat. Nanotechnol.* **3** 270
- [16] Tung V C, Chen L M, Allen M J, Wassei J K, Nelson K, Kaner R B and Yang Y 2009 Low-temperature solution processing of graphene-carbon nanotube hybrid materials for high-performance transparent conductors *Nano Lett.* **9** 1949
- [17] Becerril H A, Mao J, Liu Z, Stoltenberg R M, Bao Z and Chen Y 2008 Evaluation of solution-processed reduced graphene oxide films as transparent conductors *ACS Nano* **2** 463
- [18] Yin Z, Sun S, Salim T, Wu S, Huang X, He Q, Lam Y M and Zhang H 2010 Organic photovoltaic devices using highly flexible reduced graphene oxide films as transparent electrodes *ACS Nano* **4** 5263
- [19] Yin Z, Wu S, Zhou X, Huang X, Zhang Q, Boey F and Zhang H 2010 Electrochemical deposition of ZnO nanorods on transparent reduced graphene oxide electrodes for hybrid solar cells *Small* **6** 307
- [20] Su C Y, Lu A Y, Xu Y, Chen F R, Khlobystov A and Li L J 2011 High quality thin graphene films from fast electrochemical exfoliation *ACS Nano* doi:10.1021/nn200025p
- [21] Yoo E, Kim J, Hosono E, Zhou H, Kudo T and Honma I 2008 Large reversible Li storage of graphene nanosheet families for use in rechargeable lithium ion batteries *Nano Lett.* **8** 2277
- [22] Dong X C, Shi Y M, Huang W, Chen P and Li L J 2010 Electrical detection of DNA hybridization with single-base specificity using transistors based on CVD-grown graphene sheets *Adv. Mater.* **22** 1649
- [23] Hu W B, Peng C, Luo W J, Lu M, Li X M, Li D, Huang Q and Fan C H 2010 Graphene-based antibacterial paper *ACS Nano* **4** 4317
- [24] Mohanty N and Berry V 2008 Graphene-based single-bacterium resolution biodevice and DNA transistor: interfacing graphene derivatives with nanoscale and microscale biocomponents *Nano Lett.* **8** 4469
- [25] He Q Y, Sudibya H G, Yin Z Y, Wu S X, Li H, Boey F, Huang W, Chen P and Zhang H 2010 Centimeter-long and large-scale micropatterns of reduced graphene oxide films *ACS Nano* **4** 3201
- [26] Dan Y, Lu Y, Kybert N J, Lou Z and Johnson A T C Intrinsic response of graphene vapor sensors *Nano Lett.* **9** 1472
- [27] Wang Z, Zhou X, Zhang J, Boey F and Zhang H 2009 Direct electrochemical reduction of single-layer graphene oxide and subsequent functionalization with glucose oxidase *J. Phys. Chem. C* **113** 14071
- [28] Geringer V, Subramaniam D, Michel A K, Szafrank B, Schall D, Georgi A, Mashoff T, Neumaier D, Liebmann M and Morgenstern M 2010 Electrical transport and low-temperature scanning tunneling microscopy of microsoldered graphene *Appl. Phys. Lett.* **96** 82114

- [29] Ishigami M, Chen J H, Cullen W G, Fuhrer M S and Williams E D 2007 Atomic structure of graphene on SiO₂ *Nano Lett.* **7** 1643
- [30] Staley N, Wang H, Puls C, Forster J, Jackson T N, McCarthy K, Clouser B and Liu Y Lithography-free fabrication of graphene devices *Appl. Phys. Lett.* **90** 143518
- [31] Li X S *et al* 2009 Large-area synthesis of high-quality and uniform graphene films on copper foils *Science* **324** 1312
- [32] Li X S, Zhu Y W, Cai W W, Borysiak M, Han B Y, Chen D, Piner R D, Colombo L and Ruoff R S 2009 Transfer of large-area graphene films for high-performance transparent conductive electrodes *Nano Lett.* **9** 4359
- [33] Levendorf M P, Ruiz-Vargas C S, Garg S and Park J 2009 Transfer-free batch fabrication of single layer graphene transistors *Nano Lett.* **9** 4479
- [34] Gamo Y, Nagashima A, Wakabayashi M, Terai M and Oshima C 1997 Atomic structure of monolayer graphite formed on Ni(111) *Surf. Sci.* **374** 61
- [35] Reina A, Jia X T, Ho J, Nezich D, Son H B, Bulovic V, Dresselhaus M S and Kong J 2009 Large area, few-layer graphene films on arbitrary substrates by chemical vapor deposition *Nano Lett.* **9** 30
- [36] Kim K S, Zhao Y, Jang H, Lee S Y, Kim J M, Kim K S, Ahn J H, Kim P, Choi J Y and Hong B H 2009 Large-scale pattern growth of graphene films for stretchable transparent electrodes *Nature* **457** 706
- [37] Krauss B, Lohmann T, Chae D H, Haluska M, Von Klitzing K and Smet J H 2009 Laser-induced disassembly of a graphene single crystal into a nanocrystalline network *Phys. Rev. B* **79** 165428
- [38] Ferrari A C *et al* 2006 Raman spectrum of graphene and graphene layers *Phys. Rev. Lett.* **97** 187401
- [39] Huang Y X, Palkar P V, Li L J, Zhang H and Chen P 2010 Integrating carbon nanotubes and lipid bilayer for biosensing *Biosens. Bioelectron.* **25** 1834
- [40] Fu D and Li L J 2010 Label-free electrical detection of DNA hybridization using carbon nanotubes and graphene *Nano Rev.* **1** 5354
- [41] Ohno Y, Maehashi K, Yamashiro Y and Matsumoto K 2009 Electrolyte-gated graphene field-effect transistors for detecting pH and protein adsorption *Nano Lett.* **9** 3318
- [42] Ang P K, Chen W, Wee A T S and Loh K P 2008 Solution-gated epitaxial graphene as pH sensor *J. Am. Chem. Soc.* **130** 14392